

Neutron-hole strengths and core coupling in ^{87}Sr via the $^{88}\text{Sr}(^3\text{He},\alpha)^{87}\text{Sr}$ reaction

S. Fortier, S. Gales, E. Hourani, J. M. Maison, C. P. Massolo,* and J. P. Schapira

Institut de Physique Nucleaire, 91406 Orsay Cedex, France

(Received 5 May 1988)

Neutron-hole states in ^{87}Sr were studied by means of the $^{88}\text{Sr}(^3\text{He},\alpha)^{87}\text{Sr}$ reaction at 36 MeV. Angular distribution measurements were carried out from 3° to 41° (lab) and analyzed with the zero-range distorted-wave Born approximation method. Spectroscopic factors have been determined for about 50 discrete levels in ^{87}Sr located below 6 MeV excitation energy and for the three lowest isobaric analog states $2p_{3/2}$, $1f_{7/2}$, and $2p_{1/2}$ observed around 11 MeV. Many $l=1$ and $l=3$ discrete levels are observed in the 3–6 MeV excitation energy range. In addition, a large part of the $1f-2p$ strength is found to lie in the higher-lying continuum up to 13 MeV (about 10% and 40% for the $l=1$ and 3 contributions, respectively). The distribution of the $1f-2p$ neutron-hole strength is compared to previous data on neighboring nuclei ^{89}Zr and ^{91}Mo . In addition, angular distributions for some low-lying high-spin states in ^{87}Sr are nicely reproduced by coupled-channel calculations which assume pure two-step (inelastic plus $g_{3/2}^0$ transfer) processes. Spin-parity assignments are proposed for the levels at 1.92 MeV ($\frac{7}{2}^+$), 2.16 MeV ($\frac{11}{2}^+$), 2.55 MeV ($\frac{9}{2}^-$), and 2.60 MeV ($\frac{13}{2}^-$), on the basis of this coupled-channel analysis.

I. INTRODUCTION

Detailed investigations of several medium and heavy nuclei via one-nucleon pickup reactions have shown the existence of broad resonancelike structures at excitation energies of several MeV. These structures can be interpreted as deeply bound hole states resulting from a pickup of one nucleon from inner subshells below the Fermi surface. In particular, several neutron pickup experiments have been performed in order to localize the $1f_{7/2}$ inner-hole strength in the $N=49$ nuclei ^{89}Zr and ^{91}Mo .^{1–5} Such data are particularly useful for testing the validity of various theoretical nuclear models, based on different assumptions on the spreading mechanism of the bare-hole strength. Coupling of the hole subshells with collective states of the core⁶ has been one of the mechanisms proposed for the damping of the strength.

There has been so far no similar information available about the lighter isotone ^{87}Sr . The large amount of spectroscopic data⁷ obtained from various experiments involving nuclear reactions as well as radioactive decay mainly concerns low-lying levels below 3.5 MeV excitation energy. In the present paper we report a study of the $^{88}\text{Sr}(^3\text{He},\alpha)^{87}\text{Sr}$ reaction at 36 MeV incident energy, investigating the distribution of the $1f-2p$ neutron-hole strengths up to 12 MeV excitation energy. The experimental method is presented in Sec. II and the results of the distorted-wave Born approximation (DWBA) analysis of the data are discussed in Sec. III.

In addition, angular distributions measured for some low-lying levels in ^{87}Sr presumed to have a high spin value⁷ have been compared to the predictions of coupled-reaction-channel (CRC) calculations. The shapes of four angular distributions as well as the absolute cross sections are nicely reproduced by assuming that final states are excited through two-step processes coupling a vibrational excitation of the ^{88}Sr core and a

neutron pickup in the $1g_{7/2}^0$ orbital. These results are presented in Sec. IV, together with the J^π assignments proposed on the basis of the excellent agreement between the data and CRC predictions.

II. EXPERIMENTAL PROCEDURE

The experiment was performed using a 36-MeV ^3He beam from the Orsay MP Tandem accelerator. The outgoing α particles were analyzed by a split-pole magnetic spectrometer. The position-sensitive gas counter, using a tapped delay line system was similar to the one described in Ref. 8. It covered 50 cm of the focal plane, which allows us to observe an excitation energy range of about 15 MeV with only one setting of the magnetic field. It was backed by a proportional counter and a plastic scintillator, ensuring a ($\Delta E-E$) discrimination of different types of particles.

The 99.8% isotopically enriched ^{88}Sr target, with a thickness of about $55 \mu\text{g}/\text{cm}^2$, was prepared by vacuum evaporation of $\text{Sr}(\text{NO}_3)_2$ on a $30 \mu\text{g}/\text{cm}^2$ carbon backing. A small amount of iron contamination estimated to about 0.5% could be observed in the spectra, in addition to that due to oxygen and carbon isotopes. Angular distributions were measured at ten angles between 3° and 37° in the laboratory system, with an energy resolution typically of 25 keV for ^{87}Sr peaks. Additional measurements with a slightly better resolution (about 20 keV) were also performed for low-lying levels up to a laboratory angle of 41° with a $30 \mu\text{g}/\text{cm}^2$ thick natural strontium target, using a 1000 μm thick position-sensitive silicon detector. Independent of statistics, an overall uncertainty of about 20% is estimated for the absolute cross sections, which were deduced from a comparison of ^3He elastic scattering measurements at 13° with optical model predictions.

A typical α spectrum is displayed in Fig. 1. Fifty discrete levels or groups of levels in ^{87}Sr were identified below 6 MeV excitation energy. In addition, three

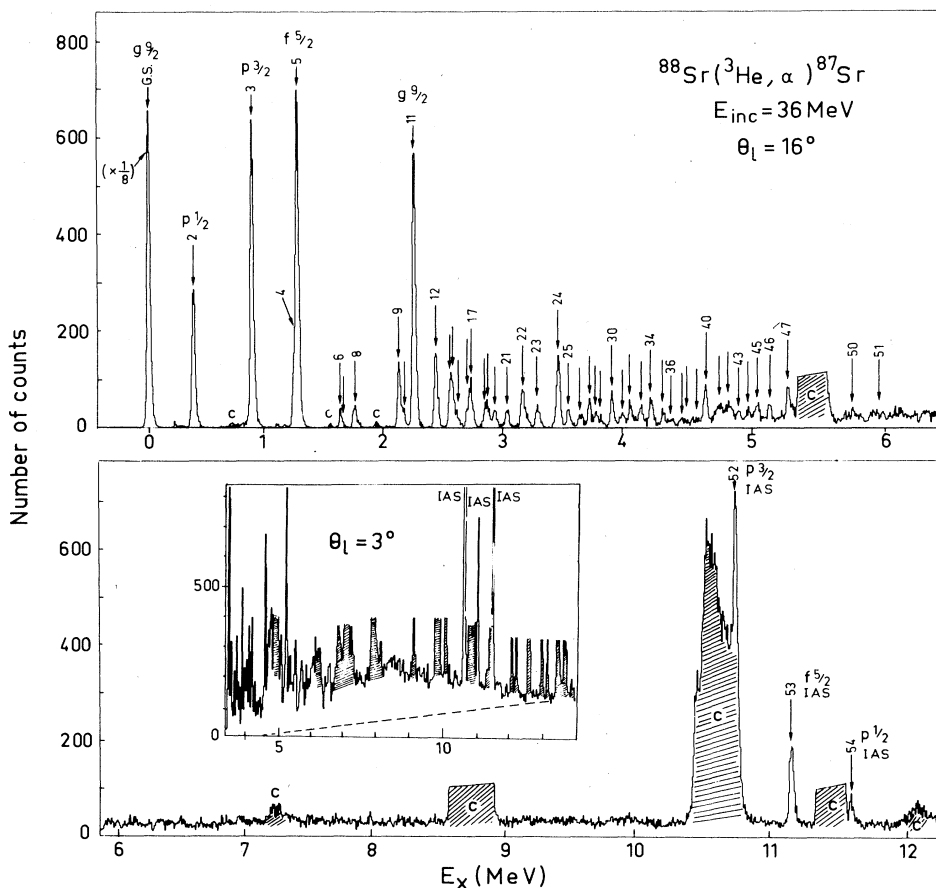


FIG. 1. Alpha spectrum at 16° (lab). The high-excitation-energy part of a spectrum at 3° is also shown in an inset, with the subtracted background (dashed line). The shaded areas are peaks due to contaminants.

discrete peaks located around 11 MeV could be identified with isobaric analog states (IAS) in ^{87}Sr , as discussed in the next section. In the case of close multiplets, the data were extracted using a multipeak fitting procedure.⁹ The excitation energies given in Table I were determined from an internal calibration procedure which used the previously known⁷ energies of some low-lying states in ^{87}Sr and those from carbon and oxygen contaminants.

Experimental angular distributions are presented in Figs. 2–6. They are compared in the next sections with the results of distorted-wave Born approximation (DWBA) and coupled-reaction-channel (CRC) calculations.

Above 6 MeV excitation energy, the density of levels increases considerably, leading to a slowly rising continuum over which peaks from various contaminants are observed. However, at all angles an inflection point or even a local minimum in the cross section can be observed at about 13 MeV, as shown for the contracted spectrum in the inset of Fig. 1. It is important to evaluate the amount of single-hole strength lying in this large structure in the continuum. The main difficulty generally encountered in the determination of high-lying single-particle or single-hole strengths in transfer reactions is related to the un-

certainly about the background to be subtracted, giving rise to large possible systematic errors. Strictly speaking, a physical background in the $(^3\text{He}, \alpha)$ spectra due to three-body reactions can be expected only above the particle emission threshold ($S_n = 8.47$ MeV in ^{87}Sr). But the empirical backgrounds chosen in most investigations of deep-hole states also implicitly include other ill-determined effects, such as those due to the excitation of the final nucleus through nondirect processes or unfavored angular-momentum transitions.

The background assumed in the present analysis is shown in Fig. 1. At each angle, it was defined by a straight line drawn from the minimum of the cross section at 13 MeV to zero at 4.5 MeV excitation energy, where peaks begin to mix due to the increasing density of levels. The differential cross sections for high-lying states in ^{87}Sr were then estimated for 1-MeV-wide energy bins in the 6–13 MeV excitation energy region. This was done by subtracting the contribution of this assumed background and that from various contaminant peaks, identified by considering their kinematic shift with angle. The corresponding angular distributions are presented in Fig. 5 with their statistical error bars, together with that measured for the assumed background.

TABLE I. Results of the analysis of the $^{88}\text{Sr}(^3\text{He},\alpha)^{87}\text{Sr}$ reaction.

N^{a}	E_x^{b} (MeV)	l	$J^{\pi^{\text{c}}}$	C^2S		$(d,t)^{\text{e}}$	$(^3\text{He},\alpha)^{\text{e}}$
				Present work ^d	$(p,d)^{\text{e}}$		
1	0	4	$\frac{9}{2}^+$	8.16	8.40	9.3	8.3
2	0.388	1	$\frac{1}{2}^-$	2.52	2.42	1.85	3.3
3	0.873	1	$(\frac{3}{2})^-$	3.36	3.91	2.71	4.0
4	1.228	(2)	$\frac{5}{2}^+$	0.17	0.43		
5	1.254	3	$\frac{5}{2}^-$	2.76	4.19	4.15	4.20
6	1.740	nd	$(\frac{13}{2}^+)$ CRC				
7	1.770	nd					
8	1.920	nd	$\frac{7}{2}^+$ CRC				
9	2.111	1	$(\frac{1}{2}, \frac{3}{2})^-$	0.63,0.54	0.66	0.35	
10	2.159	nd	$\frac{11}{2}^+$ CRC				
11	2.236	4	$\frac{9}{2}^+$	0.89	0.91	1.7	1.16
12	2.415	3	$(\frac{5}{2})^-$	0.67	0.71	0.70	
13	2.536	4	$\frac{9}{2}^+$	0.10			
14	2.554	nd	$\frac{9}{2}^-$ CRC				
15	2.596	nd	$\frac{13}{2}^-$ CRC				
16	2.679	1	$(\frac{1}{2}, \frac{3}{2})^-$	0.16,0.13		0.53	
17	2.706	4	$\frac{9}{2}^+$	0.12			
18	2.831	nd	$(\frac{15}{2}^-)$ CRC				
19	2.851	1	$(\frac{1}{2}, \frac{3}{2})^-$	0.13,0.11			
20	2.920	4	$\frac{9}{2}^+$	0.04			
21	3.020	1	$(\frac{1}{2}, \frac{3}{2})^-$	0.10,0.08			
22	3.140	3	$(\frac{5}{2}, \frac{7}{2})^-$	0.36,0.23	0.47		
23	3.260	(4)	$(\frac{9}{2}^+)$	0.08			
24	3.43	3	$(\frac{5}{2}, \frac{7}{2})^-$	0.58,0.38	0.55		
25	3.51	3	$(\frac{5}{2}, \frac{7}{2})^-$	0.15,0.10			
26	3.62	(1)	$(\frac{1}{2}, \frac{3}{2})^-$	0.08,0.07			
27	3.69	4	$\frac{9}{2}^+$	0.08			
28	3.75	4	$\frac{9}{2}^+$	0.04			
29*	3.80						
30	3.88	4	$\frac{9}{2}^+$	0.11			
31	3.96	3	$(\frac{5}{2}, \frac{7}{2})^-$	0.09,0.06			
32	4.02	4	$\frac{9}{2}^+$	0.08			
33	4.10	(3)	$(\frac{5}{2}, \frac{7}{2})^-$	0.19,0.13			
34	4.18	3	$(\frac{5}{2}, \frac{7}{2})^-$	0.26,0.17			
35	4.27	4	$\frac{9}{2}^+$	0.04			
36	4.35	(3)	$(\frac{5}{2}, \frac{7}{2})^-$	0.06,0.04			
37	4.42	1	$(\frac{1}{2}, \frac{3}{2})^-$	0.05,0.04			
38	4.47	1	$(\frac{1}{2}, \frac{3}{2})^-$	0.04,0.04			
39*	4.53	(4)	$(\frac{9}{2}^+)$	0.03			
40*	4.62	{	$(\frac{5}{2}, \frac{7}{2})^-$	0.18,0.12			
		1	$(\frac{1}{2}, \frac{3}{2})^-$	0.11,0.09			
41	4.72	3	$(\frac{5}{2}, \frac{7}{2})^-$	0.36,0.24			
42	4.78	1	$(\frac{1}{2}, \frac{3}{2})^-$	0.24,0.21			
43	4.86	1	$(\frac{1}{2}, \frac{3}{2})^-$	0.17,0.15			
44	4.95	1	$(\frac{1}{2}, \frac{3}{2})^-$	0.16,0.14			
45	5.02	3	$(\frac{5}{2}, \frac{7}{2})^-$	0.35,0.23			

TABLE I. (Continued).

N^{oa}	E_x^{b} (MeV)	l	$J^{\pi^{\text{c}}}$	C^2S		
				Present work ^d	$(p,d)^{\text{e}}$	$(d,t)^{\text{e}}$
46*	5.12	3	$(\frac{5}{2}, \frac{7}{2})^-$	0.14,0.09		
		1	$(\frac{1}{2}, \frac{3}{2})^-$	0.09,0.08		
47*	5.26	3	$(\frac{5}{2}, \frac{7}{2})^-$	0.32,0.21		
		1	$(\frac{1}{2}, \frac{3}{2})^-$	0.20,0.17		
48	5.42	3	$(\frac{5}{2}, \frac{7}{2})^-$	0.46,0.30		
49	5.56	3	$(\frac{5}{2}, \frac{7}{2})^-$	0.36,0.23		
50*	5.77	3	$(\frac{5}{2}, \frac{7}{2})^-$	0.54,0.35		
51*	5.92	3	$(\frac{5}{2}, \frac{7}{2})^-$	0.26,0.17		
		6-7	$(\frac{5}{2}, \frac{7}{2})^-$	1.72,1.12		
		1	$(\frac{1}{2}, \frac{3}{2})^-$	0.24,0.21		
		3	$(\frac{5}{2}, \frac{7}{2})^-$	1.86,1.21		
		1	$(\frac{1}{2}, \frac{3}{2})^-$	0.51,0.44		
		3	$(\frac{5}{2}, \frac{7}{2})^-$	1.95,1.27		
		1	$(\frac{1}{2}, \frac{3}{2})^-$	0.28,0.24		
		3	$(\frac{5}{2}, \frac{7}{2})^-$	1.39,0.90		
		1	$(\frac{1}{2}, \frac{3}{2})^-$	0.25,0.21		
		3	$(\frac{5}{2}, \frac{7}{2})^-$	0.73,0.47		
		1	$(\frac{1}{2}, \frac{3}{2})^-$	0.20,0.17		
		3	$(\frac{5}{2}, \frac{7}{2})^-$	0.42,0.27		
		1	$(\frac{1}{2}, \frac{3}{2})^-$	0.14,0.12		
52	10.72	1	$\frac{3}{2}^-, T = \frac{13}{2}$	0.50 (IDP = 0.31)		
53	11.12	3	$\frac{5}{2}^-, T = \frac{13}{2}$	1.00 (IDP = 0.53)		
54	11.55	1	$\frac{1}{2}^-, T = \frac{13}{2}$	0.24 (IDP = 0.15)		

^aThe numbers are those labeling the peaks observed in the spectrum of Fig. 1. The symbol * indicates the presence of an unresolved multiplet.

^bUncertainties on excitation energies are estimated to be lower than 10 keV below 4 MeV, and about 20 keV for higher-lying levels.

^cFrom Ref. 7 for previously known J^{π} values. For levels with nondirect (nd) angular distributions, the J^{π} assignment results from the present CRC analysis.

^dSee text.

^eReference 7.

III. DWBA ANALYSIS

A. Calculations

Zero-range DWBA calculations were performed with the code DWUCK4.¹⁰ The form factors for the transferred neutron were calculated with the standard procedure, by adjusting the depth of the Woods-Saxon well in order to reproduce the experimental binding energy. The geometrical parameters of the potential well are given in Table II.

However, as this method is known to give poor results for transitions to IAS because in this case the effect of the isospin-dependent part of the nuclear potential cannot be neglected, the form factors for the IAS were also calculated according to the procedure first proposed by Stock and Tamura.¹¹ An isospin-coupling term proportional to $t \cdot T$ (Lane potential) was added to the usual isoscalar potential (cf. Table II): the neutron form factors for the

IAS are then obtained after an appropriate normalization by numerically solving¹¹ the Lane coupled equations resulting from the additional term.

The results of calculations using various sets of optical potentials for both entrance and exit channels have been compared to the experimental angular distributions obtained for the lowest $1g_{7/2}^{\frac{3}{2}}$, $2p_{1/2}^{\frac{1}{2}}$, and $1f_{7/2}^{\frac{5}{2}}$ hole states located at 0, 0.388, and 1.254 MeV excitation energies, respectively. The C^2S values were then deduced by means of the expression

$$C^2S = \frac{(2j+1)\sigma_{\text{expt}}}{N\sigma_{\text{DW}}^{ij}}, \quad (1)$$

where j is the total angular momentum of the transferred particle and σ_{DW}^{ij} the cross section predicted by the DWBA calculation. The normalization factor N has been taken as equal to the commonly adopted value of 23.

The set of ^3He and α potentials finally adopted is given

in Table II, labeled as *A1-B1*. It was previously used in the analysis of the $^{92}\text{Mo}(^3\text{He},\alpha)^{91}\text{Mo}$ reaction⁴ at 25 MeV incident energy, and in the present case gave the best overall agreement with experiment for the three different l values. The results obtained with other sets of optical potentials generally give poorer agreement with experimental data, with a variation of C^2S values for the different l transfers typically within 20%. As an example, the results obtained with the set labeled *A2-B2* in Table II, which was used in the analysis of the $^{90}\text{Zr}(^3\text{He},\alpha)^{89}\text{Zr}$ reaction¹ at 39 MeV are shown for comparison.

Finite-range DWBA calculations were also performed on the same three states, using the code DWUCK5.¹⁰ Theoretical shapes of angular distributions as well as ratios of spectroscopic factors for different l values were found to be very similar to those from zero-range calculations. Therefore the following analysis of the present data was done using the zero-range approximation.

B. Results

Experimental angular distributions have been compared to DWBA predictions, leading to l assignments for most discrete ^{87}Sr levels identified in this experiment. In Figs. 3 and 4 the results for $l=4, 3$, and 1 transfers are displayed, corresponding to the neutron pickup in the

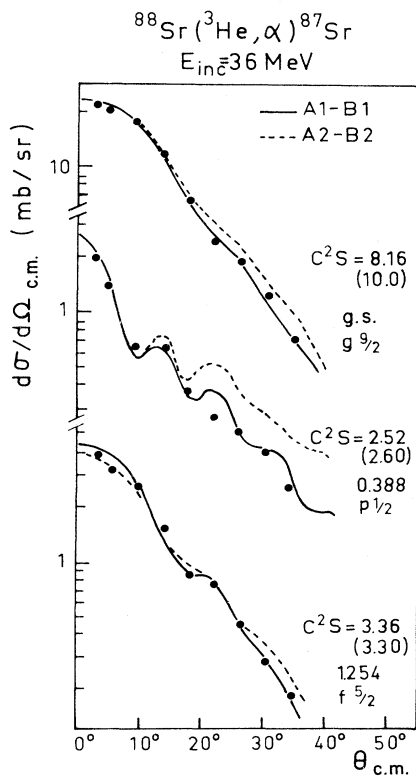


FIG. 2. Comparison of experimental angular distributions with DWBA predictions, for two different sets of ^3He and α optical potentials reported in Table II. The C^2S values within parentheses correspond to the calculation done with parameters *A2-B2* (dotted line).

$1g_{7/2}^+$ and $1f-2p$ orbitals. The experimental shapes are generally well reproduced by DWBA calculations without any ambiguity on the value of the transferred angular momentum. In particular, the good statistics of the present data allows an easy discrimination between $l=3$ and $l=4$ transfers, as can be seen in Fig. 3. On the other hand, the angular distribution observed in Fig. 3 for the known $5/2^+$ level at 1.23 MeV is only poorly reproduced

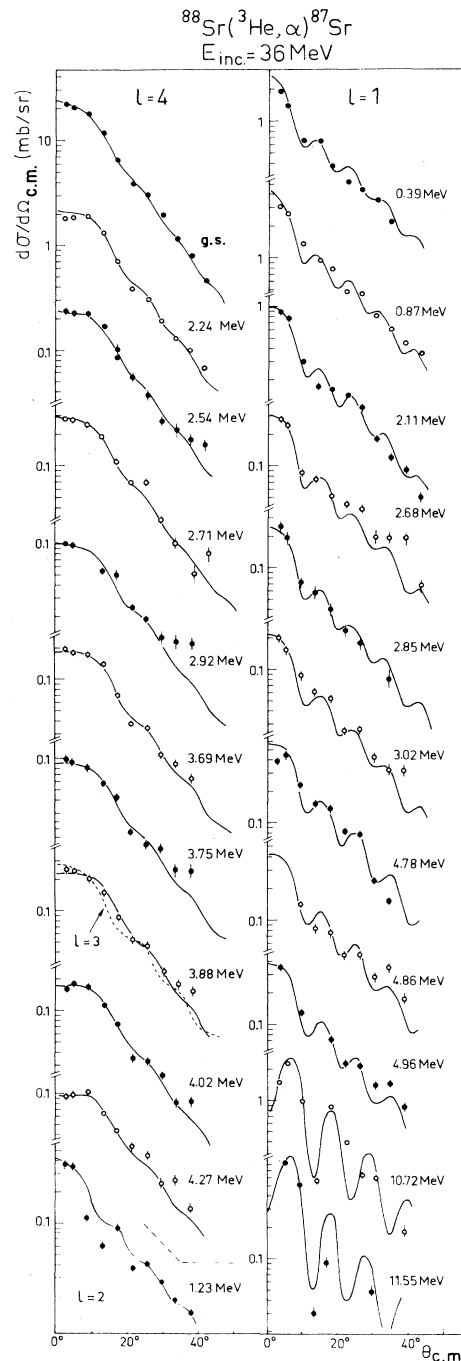


FIG. 3. Comparison of experimental angular distributions with DWBA predictions (see text).

the $l=2$ DWBA prediction. Such an excitation is expected to proceed through small amounts of $2d_{5/2}$ admixtures in the wave function of the ^{88}Sr ground state. Three angular distributions corresponding to multiplets of levels could be reproduced by the addition of $l=1$ and $l=3$ transfers, with relative strengths determined by the least-squares method.

The same least-squares method was also applied for the 1 MeV energy bins in the high-energy continuum up to

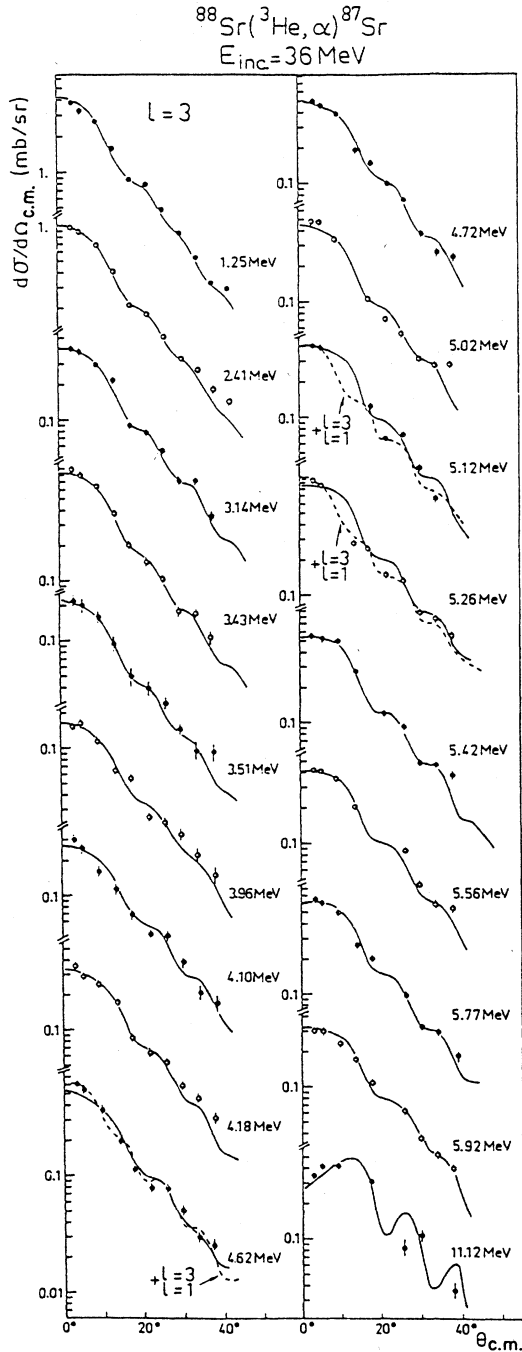


FIG. 4. Same as Fig. 3.

12 MeV. The results are displayed in Fig. 5. The slightly oscillating angular distributions could only be reproduced by a mixing of $l=1$ and $l=3$ transfers, corresponding to a neutron pick-up in the inner f - p shell. It was not possible to observe any $l=2$ contribution corresponding to a pickup in the more internal $1d_{5/2}$ orbital. Slightly different assumptions about the background lead to the same qualitative conclusions. Between 12 and 13 MeV, a small cross section with large error bars did not allow us to extract the relative contribution of $l=1$ and $l=3$ strengths. The corresponding spectroscopic strengths have been neglected in the following discussion, as the cross section was found to be less than a third of that measured for the 11–12 MeV bin.

The l values and the spectroscopic strengths C^2S deduced from this analysis are listed in Table I. All $l=4$ transitions are assumed to correspond to $\frac{9}{2}^+$ final levels, from arguments based on the shell model. For $l=1$ and $l=3$ transitions corresponding to levels with unknown spin values, the C^2S values are given for the two possible

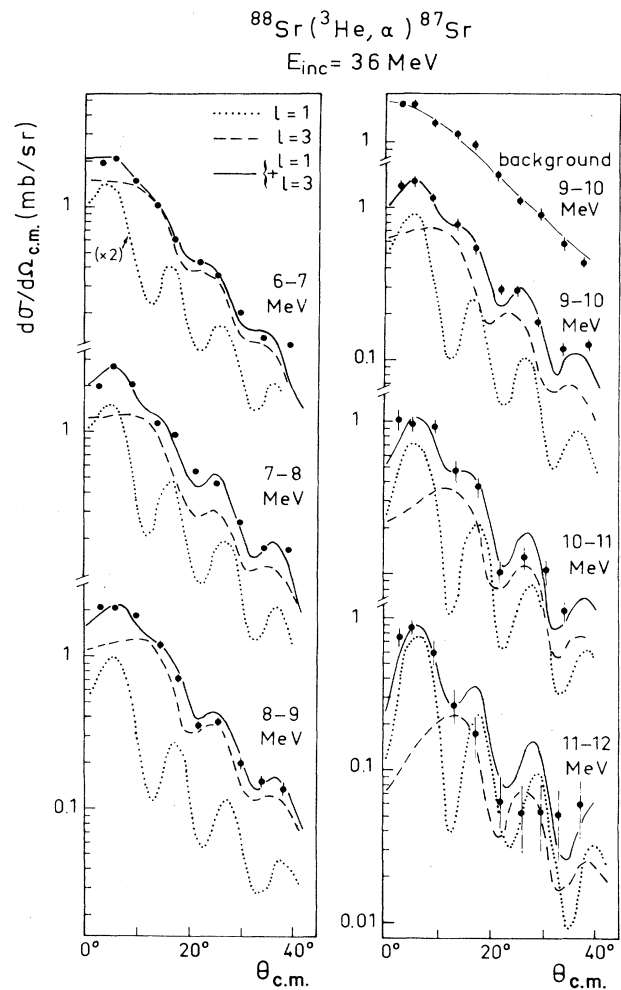


FIG. 5. Experimental angular distributions for 1-MeV-wide excitation energy bins between 6 and 12 MeV in ^{87}Sr , compared with DWBA predictions for a sum of $l=1$ and $l=3$ transfers.

spin values $l + \frac{1}{2}$ and $l - \frac{1}{2}$. They differ by 13% and 33% for $l = 1$ and $l = 3$, respectively.

1. Isobaric analog states

The three narrow peaks observed at 10.72, 11.12, and 11.55 MeV may be identified with those reported at about the same excitation energies in a study of the (p, d) reaction¹³ and proposed to be $T = \frac{13}{2}$ states, isobaric analogs of the ground and first two excited states of ^{87}Rb . Their angular distributions are well reproduced by DWBA pre-

dictions for $l = 1, 3$, and 1 , respectively, in good agreement with the proposed $\frac{3}{2}^- - \frac{5}{2}^-$, and $\frac{1}{2}^-$ spin and parity assignment. Higher-lying IAS could not be unambiguously identified in the present experiment, because of the large number of contaminant peaks present in the high-excitation-energy part of the spectra. The spectroscopic strengths determined for the IAS using the isospin-dependant procedure (IDP) are strongly reduced compared with those obtained from the standard separation energy procedure, as shown in Table I. Such a reduction of the C^2S values is consistent with what was observed in other nuclei.¹⁴ The resulting values are then in good agreement with the sum-rule limits for $T = \frac{13}{2}$ components, which are given in Table III.

2. Summed spectroscopic strengths and distribution of neutron-hole states

The shell-model sum rules for $T = \frac{11}{2}$ states are also compared in Table III with the summed spectroscopic strengths $\sum C^2S$ measured for $l = 1, 3$, and 4 transitions to discrete levels and to the continuum region between 6 and 12 MeV excitation energy. Two extremum values are given in Table III for the $l = 1$ and $l = 3$ summed strengths for discrete levels, corresponding to the opposite assumptions that all transitions with unknown transferred spin be either $j = l + \frac{1}{2}$ or $j = l - \frac{1}{2}$. As the experimental values for $l = 1$ and $l = 3$ transitions below 6 MeV exhaust the shell-model predictions for $2p_{\frac{1}{2}}$ and $1f_{\frac{5}{2}}$ subshells, the $l = 1$ and $l = 3$ strengths above this energy were then assumed to correspond only to the deeper $2p_{\frac{3}{2}}$ and $1f_{\frac{7}{2}}$ orbitals.

The summed spectroscopic strengths are discussed below for the different l values. The distribution of $l = 1, 3$, and 4 strengths with respect to excitation energy are displayed in Fig. 6, using 1-MeV-wide energy bins. In a more detailed way, the fragmentation of the neutron-hole states over discrete levels is also shown in Fig. 6, corresponding to the C^2S values of Table I. In this figure the unknown transferred j values have been arbitrarily assumed to be equal to $l + \frac{1}{2}$ above 0.8 and 5 MeV for $l = 1$ and 3 , respectively, whereas the $j = l - \frac{1}{2}$ assumption has been made for levels at lower energies.

(a) $l = 4$ transitions. The $1g_{\frac{9}{2}}$ summed strength for all $l = 4$ fragments is in excellent agreement with the shell-model sum rule. The main part of the $1g_{\frac{9}{2}}$ neutron-hole strength is concentrated in the ground state (83%) and to a lesser extent in the 2.236 MeV level (9%). The remaining $1g_{\frac{9}{2}}$ strength has been observed to be shared between ten levels located between 2.5 and 4.5 MeV excitation energy. The centroid of the $1g_{\frac{9}{2}}$ strength deduced from the present experiment is 0.45 MeV.

(b) $l = 1$ transitions. The summed strength for $l = 1$ transitions determined in the present analysis is much larger than the shell-model sum rule for $2p_{\frac{1}{2}}$ and $2p_{\frac{3}{2}}$, exceeding it by at least 57%. It can be noticed that the C^2S value determined for the lowest $\frac{1}{2}^-$ state at 0.388 MeV already exceeds the $2p_{\frac{1}{2}}$ sum rule by 36%. These anomalously large values of $l = 1$ spectroscopic factors compared to those found for $l = 3$ and $l = 4$ transitions in

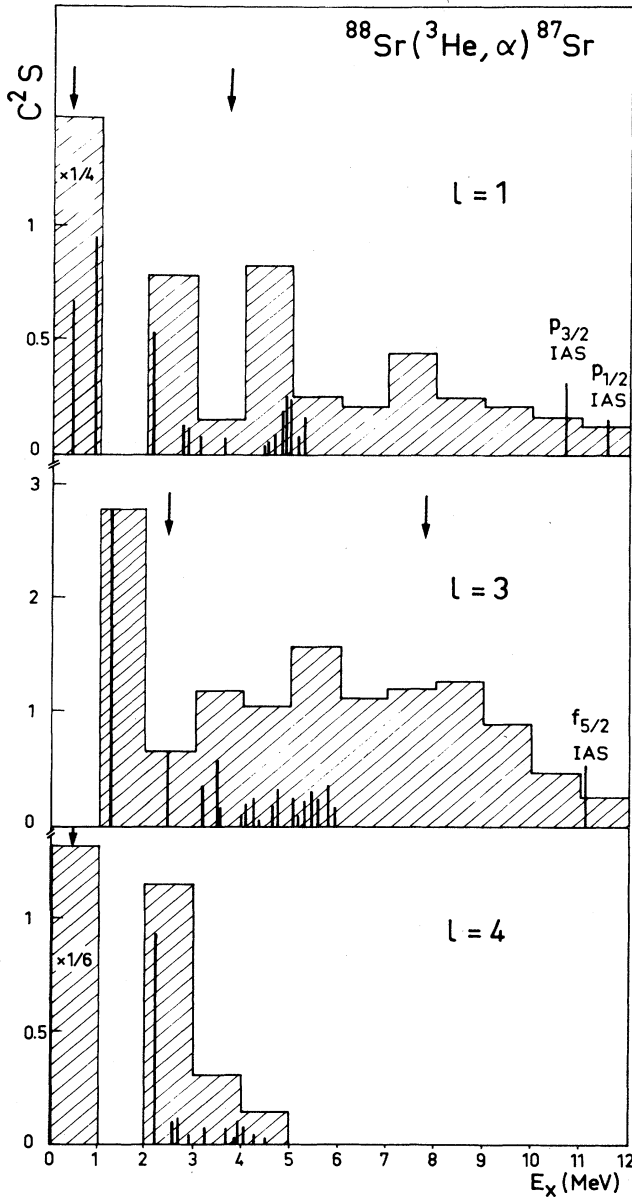


FIG. 6. Distribution of $l = 1, 3$, and 4 neutron-hole strengths in ^{87}Sr relative to excitation energy (hatched areas). Spectroscopic factors of discrete levels are represented with vertical bars. The arrows indicate the position of $T = \frac{11}{2}$ energy centroids for $j = l + \frac{1}{2}$ and $j = l - \frac{1}{2}$ strengths deduced from the present data (see text).

TABLE II. Optical model parameters^a used in the analysis of the $^{88}\text{Sr}(^3\text{He},\alpha)^{87}\text{Sr}$ reaction.

Channel	V	r_0	a	W	r'_0	a'	V_c	
^3He	$A1$	152.6	1.20	0.72	35.8	1.40	0.88	1.3
	$A2$	175	1.14	0.72	17.5	1.60	0.81	1.3
α	$B1$	207	1.30	0.65	28	1.30	0.52	1.4
	$B2$	206	1.41	0.52	25.8	1.41	0.52	1.3
n	U_0		1.25	0.65				

^aReference 12. The potentials for ^3He and α were of the form

$$V(r) = v_c - Vf(r, r_0 A^{1/3}, a) - iWf(r', r'_0 A^{1/3}, a'),$$

where $f(r, r_0 A^{1/3}, a) = (1 + \exp[r - (r_0 A^{1/3})]/a)^{-1}$ and V_c is the Coulomb potential. The form factors are computed with a binding potential:

$$U(r) = -U_0 \left[f(r, r_0 A^{1/3}, a) - \frac{0.55}{r} \frac{d}{dr} f(r, r_0 A^{1/3}, a) \text{LS} \right].$$

For IAS, an isospin-dependent potential of the form $(4U_1/A)\text{tT}$ is added to the binding potential:

$$U_1 = -V'_1 a \frac{d}{dr} f(r, r_0 A^{1/3}, a)$$

with $V'_1 = 117$ MeV.

the present analysis are not well understood, but could be due to the poor matching of angular momenta for low- l transfer in the $(^3\text{He},\alpha)$ reaction [the value of $(k_f - k_i)R$ is about 4.2 at 1 MeV and 2.0 at 10 MeV]. Examples of such problems encountered in DWBA analyses are often found in the comparison of results from different one-nucleon transfer reactions leading to the same final nucleus. In particular, the comparison with previous results from one-neutron pickup reactions on ^{88}Sr presented in Table I shows strong discrepancies in the relative values of spectroscopic factors for different l transfers. This doubt about the validity range of the absolute value of the $l=1$ spectroscopic strengths determined by the DWBA method, which appears to exceed the generally accepted 20% uncertainty, should not affect the determination of relative values, as long as two-step processes can be neglected. Thirteen $l=1$ levels are observed between 2 and 6 MeV, carrying about 20% of the sum of

the spectroscopic factors measured for the lowest $\frac{1}{2}^-$ and $\frac{3}{2}^-$ states at 0.388 and 0.873 MeV.

By assuming that the whole $2p_{\frac{1}{2}}$ strength is concentrated in the known $\frac{1}{2}^-$ level at 0.388 MeV, the centroid energy of the $2p_{\frac{3}{2}}$ strength deduced from the present data is 3.7 MeV. The corresponding value of 3.3 MeV for the energy gap between the $2p_{\frac{1}{2}}$ and $2p_{\frac{3}{2}}$ neutron-hole states in ^{87}Sr is probably slightly overestimated as some of the $l=1$ levels observed in the present $(^3\text{He},\alpha)$ experiment could have a spin value of $\frac{1}{2}$, and additional spin measurements would be necessary for a more precise determination. However, the striking result obtained about the $2p_{\frac{3}{2}}$ strength is that it is diluted over a large range of excitation energy, even if about half of the total measured strength is concentrated onto the lowest fragment at 0.873 MeV.

TABLE III. Comparison of summed spectroscopic strengths $\sum C^2S$ from the DWBA analysis of the $^{88}\text{Sr}(^3\text{He},\alpha)^{87}\text{Sr}$ reaction, with the shell-model (SM) sum rules.

lj	$T = \frac{13}{2}$		SM	$T = \frac{11}{2}$		
	SM	Present work		(0-6 MeV)	Present work ^b (6-12 MeV)	(0-12 MeV)
$g_{9/2}$	0		10	9.77		9.77
$f_{5/2}$	0.46	0.53 ^a	5.54	12.92	6.50 → 8.09	11.74 → 13.33
$f_{7/2}$	0.62		7.38			
$p_{1/2}$	0.15	0.15 ^a	1.85	5.54	7.33 → 8.04	9.72 → 10.43
$p_{3/2}$	0.31	0.31 ^a	3.69			

^a C^2S values for IAS deduced from the IDP procedure (see text).

^bThe minimum and maximum values quoted for $\sum C^2S$ in the 0-6 MeV region correspond to assumed $j=l+\frac{1}{2}$ and $j=l-\frac{1}{2}$ transfers, respectively, in the case of levels with previously unknown J^π values.

(c) $l=3$ transitions. Depending on the spin value assumed for the transitions, the range of values deduced from the present analysis for the summed $l=3$ spectroscopic strengths extends from 91 to 103% of the shell-model prediction for the sum of $1f_{\frac{5}{2}}$ and $1f_{\frac{7}{2}}$ strengths. This good agreement with the shell-model sum rule leads to the conclusion that the $1f$ strength in ^{87}Sr is practically exhausted below 13 MeV excitation energy, where a local minimum of the ($^3\text{He},\alpha$) cross section has been observed.

A reliable estimation of the centroid energies of the $1f_{\frac{5}{2}}$ and $1f_{\frac{7}{2}}$ neutron-hole strengths would need measurements of the transferred spin. However, by using the same previous assumptions that $1f_{\frac{5}{2}}$ levels are mainly located below 5 MeV (as the $1f_{\frac{5}{2}}$ strength is exhausted in this region) and that other $l=3$ levels at higher energy have spin $\frac{7}{2}$, tentative values of 2.4 and 7.7 MeV are obtained for the value of centroid energies of the $1f_{\frac{5}{2}}$ and $1f_{\frac{7}{2}}$, $T=\frac{1}{2}$ neutron-hole states. A value of 5.3 MeV is then proposed for the $1f$ spin-orbit splitting of $T=\frac{1}{2}$ states in ^{87}Sr .

It is clearly difficult to give an estimate of the accuracy on this splitting value, which is mainly derived from two basic assumptions: (i) the $f_{\frac{7}{2}}$ strength is exhausted below 12 MeV; (ii) all $l=3$ states below 5 MeV have spin $\frac{5}{2}$. The splitting value would have to be decreased by a different distribution of spin values $\frac{5}{2}$ and $\frac{7}{2}$ between the various $l=3$ levels, which is quite likely. On the other hand, it would have to be increased if some noticeable part of the $1f_{\frac{7}{2}}$, $T=\frac{1}{2}$ strength lies above 12 MeV. In fact, the summed $1f_{\frac{7}{2}}$ strength amounts to 92% of the sum rule, with the $\frac{5}{2}$ - $\frac{7}{2}$ distribution assumed above and the present hypothesis about the background. Other reasonable background assumptions could decrease or increase this summed strength by a few percent and, consequently, the presence of some higher-lying $1f_{\frac{7}{2}}$, $T=\frac{1}{2}$ strength increasing the splitting value cannot be excluded. Considering the possible compensation of the systematic errors from assumptions (i) and (ii), it is hoped that the value of 5.3 MeV proposed for the spin-orbit splitting of the $1f$, $T=\frac{1}{2}$ strength is not too unreliable.

C. Comparison with ^{89}Zr and ^{91}Mo data

Experimental results about high-lying neutron-hole states in the neighboring $N=49$ nuclei can be quoted here for comparison. Relevant data in ^{89}Zr have been obtained by means of the ($^3\text{He},\alpha$) reaction at 39 MeV,¹ 205 MeV,² and 97 MeV (Ref. 3) and from a study of the (p,d) reaction at 90 MeV.⁵ Similar data about ^{91}Mo are from studies of the ($^3\text{He},\alpha$) reaction at 97 MeV (Ref. 3) and 25 MeV (Ref. 4).

The main purpose of the experiments reported in Refs. 2, 3, and 5 was to search for $1f_{\frac{7}{2}}$ neutron-hole excitations, taking advantage of the known selectivity of pickup reactions at relatively high incident energies ($E \geq 90$ MeV) for large values of transferred angular momentum. Spectra measured up to 25 MeV excitation energy in ^{89}Zr

from both ($^3\text{He},\alpha$) and (\bar{p},d) reactions display the same pattern: In addition to the well-known low-lying valence states, a concentration of discrete levels with transferred angular momentum $l=3$ is observed between 3 and 7 MeV excitation energy. At higher energy, narrow peaks identified as the isobaric analog states of ^{89}Y low-lying levels are located over a broad asymmetric structure, which is itself superimposed over a large continuum background. This structure can be roughly divided into two parts, a bump located between 7 and 12 MeV with an angular distribution consistent with an $l=3$ assignment, and a tail extending up to 20 MeV. Similar concentrations of $l=3$ pick-up strengths at the same excitation energies are also observed in the $^{92}\text{Mo}(^3\text{He},\alpha)^{91}\text{Mo}$ spectra.³ Excitation energies in ^{87}Sr above 15 MeV have not been investigated, but it can be noticed that a minimum at about 12 MeV is observed in the distribution of the $l=3$ strength, as in the other $N=49$ isotones.

A quantitative comparison of spectroscopic strengths is particularly delicate for high-lying states embedded in a continuum, as large but rather ill-determined errors can come from the background subtraction procedure and from the DWBA analysis itself. It was first proposed in Ref. 3 that about half of the $1f_{\frac{7}{2}}$, $T_{<}$ strength in ^{89}Zr could be contained in the $l=3$ discrete levels observed between 3 and 7 MeV, 15% of the strength lying in the 7–12 MeV bump. However, results obtained from the (\bar{p},d) reaction⁵ have shown that the $l=3$ strength below 7 MeV was mainly due to the excitation of residual $1f_{\frac{5}{2}}$ fragments. From their analysis, it was deduced that only 15% of the total $1f_{\frac{7}{2}}$ shell-model strength can be found in this low-energy region, whereas 35 and 25% of the strength would lie in the 7–12 and 12–16 MeV excitation energy regions, respectively. Although the present data about the $l=3$ strength in ^{87}Sr only concern the region below 12 MeV, and do not allow us to discriminate between $1f_{\frac{5}{2}}$ and $1f_{\frac{7}{2}}$ excitation, the DWBA analysis indicates that the $1f_{\frac{7}{2}}$, $T=\frac{1}{2}$ hole strength is practically exhausted below 12 MeV and an approximate value of 5.3 MeV has been proposed for the energy shift between the centroids of the $1f_{\frac{5}{2}}$ and $1f_{\frac{7}{2}}$, $T_{<}$ states. This value is close to the 5.1 MeV spin-orbit splitting of $1f$ proton orbits determined from a study of the $^{90}\text{Zr}(d,^3\text{He})^{89}\text{Y}$ reaction,¹⁵ and in agreement with theoretical expectations,⁶ but appreciably lower than the 7 MeV value deduced for neutron orbits from the $^{90}\text{Zr}(\bar{p},d)^{89}\text{Y}$ experiment.⁵ It is not clear whether these differences between the quantitative results in ^{87}Sr and ^{89}Zr are significant or only due to the uncertainties accumulated in the different steps of the data analyses in both experiments.

Information about high-lying $l=1$ states has been obtained only in the case of ^{91}Mo , from the low-incident-energy data of Ref. 4, and unfortunately it was limited to discrete levels below 6 MeV excitation energy. A strong fragmentation of the $2p_{\frac{1}{2}}$ and $2p_{\frac{3}{2}}$ strength has been observed in this nucleus, with about 15 $l=1$ levels in the 2–6 MeV region, carrying about 15% of the $l=1$ neutron-hole strength present in the lowest $\frac{1}{2}^-$ and $\frac{3}{2}^-$ states at 0.653 and 1.156 MeV. This situation is quite similar to what is observed here for discrete levels in ^{87}Sr .

Several weak $l=4$ levels have been observed in the 2–4.5 MeV excitation energy region in both ^{89}Zr (Ref. 1) and ^{91}Mo (Ref. 4) nuclei. Their summed spectroscopic strengths amount to about 6 and 8 %, respectively, of the total $1g_{7/2}^9$ strength which is mainly concentrated in the ground state and in the second $\frac{9}{2}^+$ state (at 1.52 MeV in ^{89}Zr and 1.90 MeV in ^{91}Mo). Similar features of the fragmentation of the $1g_{7/2}^9$ strength in ^{87}Sr are observed in the present work.

In conclusion, ^{87}Sr appears to be rather similar to the other $N=49$ isotones, at least in a qualitative way. A theoretical calculation has been done in the framework of the phonon-quasiparticle coupling model,⁶ predicting the distribution of the $1f_{7/2}^5$ and $1f_{7/2}^7$ neutron-hole strengths in both ^{89}Zr and ^{91}Mo . It would be of interest to do similar calculations in ^{87}Sr , for comparison with the present data.

IV. CRC ANALYSIS

Most angular distributions measured in the present reaction have been correctly reproduced by DWBA calculations, which assume a direct mechanism for the neutron transfer. However, a few levels located below 3 MeV display quite different shapes of angular distributions, which could be explained by the occurrence of nondirect reaction mechanisms. These levels (which are labeled “nd” in Table I) had been previously observed in a study of the $^{86}\text{Kr}(\alpha, n\gamma)^{87}\text{Sr}$ reaction.¹⁶ They have been tentatively identified^{6,16} with high-spin members of weak-coupling multiplets resulting from the coupling of a $g_{7/2}^9$ neutron hole with the lowest 2^+ and 3^- vibrational states in ^{88}Sr , located at 1.84 and 2.73 MeV, respectively. A direct transfer is in fact expected to be strongly inhibited for ^{87}Sr high-spin states with J^π values such as $\frac{11}{2}^+$, $\frac{13}{2}^+$, $\frac{13}{2}^-$, and $\frac{15}{2}^-$, as the presence of weak $i_{11/2}^1$, $i_{13/2}^1$, $j_{13/2}^1$, and $j_{15/2}^1$ hole components in the wave function of the ^{88}Sr ground state should be very unlikely from simple shell-model considerations. Alternatively, these high-spin states can be easily excited via a two-step mechanism involving an inelastic excitation of the ^{88}Sr core followed by or preceded by a neutron pickup from the $1g_{7/2}^9$ orbital. This was first noticed in Ref. 17, where the two-step excitation of core-coupled states in ^{87}Sr was specially investigated in a study of the $^{88}\text{Sr}(p, d)^{87}\text{Sr}$ reaction at 27 MeV incident energy.

Therefore, experimental angular distributions with a nondirect character have been compared with the results of CRC calculations for pure two-step transitions, using the crude assumption of the weak-coupling model for the structure of the final levels, assumed to be members of the $(2^+ \otimes g_{7/2}^9)^{-1}$ and $(3^- \otimes g_{7/2}^9)^{-1}$ multiplets. In this case, the theoretical differential cross sections result from the interference of only two reaction paths, corresponding to an inelastic excitation process either in the entrance or the exit channel. In addition, the inelastic couplings were assumed to be only one-way. The corresponding coupling scheme is shown in Fig. 7. These calculations were performed using the code CHUCK2,¹⁰ with the same optical potentials and prescriptions for form factors and normalization as those used in the DWBA analysis. Spectro-

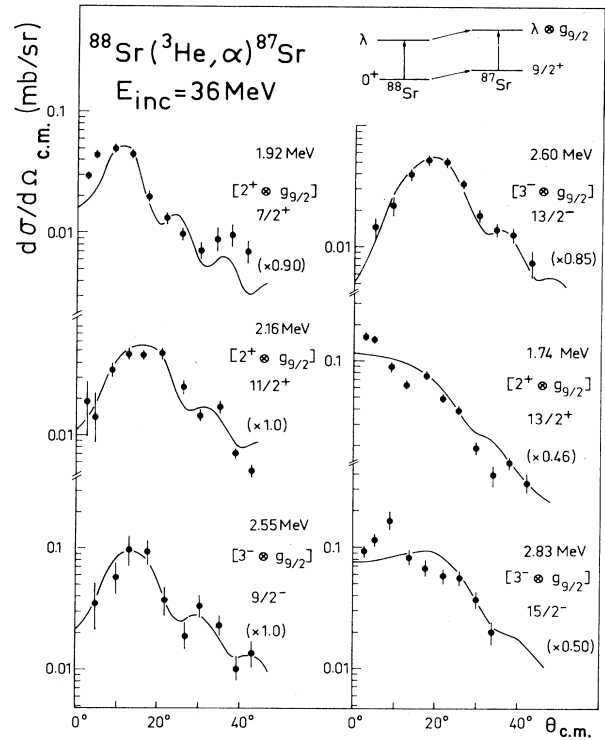


FIG. 7. Comparison of experimental angular distributions with CRC predictions for a pure two-step excitation of core-coupled states in ^{87}Sr .

scopic amplitudes used for the $1g_{7/2}^9$ transfers corresponded to a spectroscopic factor of 10. The deformation parameters for the 2^+ and 3^- states were taken equal to the values 0.11 and 0.17, from the results of a (p, p') experiment.¹⁸

The shapes of the calculated two-step angular distributions have been found to be strongly dependent on the spin and parity of the final level, in agreement with previous results obtained in a study of the $(^3\text{He}, \alpha)$ reaction on several nuclei in the $f_{7/2}^7$ shell.¹⁴ In particular, bell-shaped angular distributions with the position of the first maximum increasing in angle with the final spin value are obtained for transitions to $(J_{\text{max}}-1)$ and $(J_{\text{max}}-3)$ members of the multiplets. The experimental differential cross sections for the levels at 1.92, 2.16, 2.55, and 2.60 MeV are in remarkable agreement with the predictions for final J^π values of $\frac{7}{2}^+$, $\frac{11}{2}^+$, $\frac{9}{2}^-$, and $\frac{13}{2}^-$. The calculated angular distributions normalized to the data are shown in Fig. 7. The normalization factors for these four levels do not differ from 1 by more than 15%, which is quite satisfactory considering the crude approximations made in the CRC calculation. Spin and parity assignments can therefore be tentatively proposed from the present analysis. One can notice that they are in agreement with those proposed in Ref. 16 for the same levels, which were based on γ - γ angular correlation results with the additional assumption of having observed cascades along the yrast line. The present results obtained in a completely different way strongly support the previous assump-

tions^{6,16} about the core-excited structure and spin and parity values of the levels at 1.92, 2.16, 2.55, and 2.60 MeV.

On the other hand, J^π values of $\frac{13}{2}^+$ and $\frac{15}{2}^-$, respectively, have been proposed in Ref. 16 for the levels at 1.74 and 2.83 MeV, which could then be the J_{\max} components of the $(2^+ \otimes g_{\frac{9}{2}}^{-1})$ and $(3^- \otimes g_{\frac{9}{2}}^{-1})$ weak-coupling multiplets. In such a case the differential cross sections calculated for these spin values are stronger than the experimental ones by a factor of about 2 and do not reproduce the oscillatory shape experimentally observed for these two levels (cf. Fig. 7). It can be noticed that similar disagreements between CRC calculations and data for the J_{\max} members of multiplets had been previously observed in $f_{\frac{7}{2}}$ shell nuclei.¹⁴ However, as the proposed assignments¹⁶ are only tentative, it is not possible to draw any definite conclusion about the range of validity of these extremely schematic coupled-channel calculations, which in particular neglect the effects of Pauli blocking.

The present results can be compared to those obtained in the study of the (p,d) reaction at 27 MeV.¹⁷ Coupled-channel calculations using the same assumption of weak coupling as in the present work have been performed¹⁷ for the (p,d) excitation of the $(2^+ \otimes g_{\frac{9}{2}}^{-1})$ states with $J^\pi = \frac{7}{2}^+, \frac{11}{2}^+, \text{ and } \frac{13}{2}^+$. Although the detailed shapes of the experimental (p,d) angular distributions are not accurately reproduced, the predicted two-step cross sections are found to be in good agreement with the data,¹⁷ assuming spin values of $\frac{7}{2}, \frac{11}{2}, \text{ and } \frac{13}{2}$ for the levels at 1.92, 2.16, and 1.74 MeV, respectively. It can be noticed that the two-step (p,d) cross sections are weaker than the corresponding $(^3\text{He},\alpha)$ ones by factors from about 3 to 10, with only a weak spin dependence of the shapes of angular distributions. Therefore, the $(^3\text{He},\alpha)$ reaction with its larger sensitivity to two-step processes appears to be better adapted for the investigation of high-spin core-excited states.

One-step excitations of low-spin members of weak-coupling multiplets are expected to compete with two-step processes, through configuration mixing in the wave functions of the initial and final states. The $\frac{9}{2}^+$ level at 2.24 MeV, presumed to be the $J = \frac{9}{2}$ component of the $(2^+ \otimes g_{\frac{9}{2}}^{-1})$ multiplet,⁶ displays an angular distribution well reproduced by a direct $l=4$ transfer. The corresponding $J = \frac{5}{2}$ core-excited strength could be shared between the two $\frac{5}{2}^+$ levels at 1.23 and 1.77 MeV. A detailed investigation of possible mixing of two-step processes with direct $l=2$ transfer was beyond the scope of the present paper, but some improvement of the fit to the data could be expected for these levels by taking both direct and nondirect processes into account. In a more

general way, further CRC analyses should use detailed wave functions from structure calculations, and thus test the validity of different models (there have been, so far, several calculations about low-lying levels in ^{87}Sr , using the unified model^{19,20} and the particle-core coupling model²¹).

V. SUMMARY

A large amount of new spectroscopic data has been obtained about ^{87}Sr by means of the present $(^3\text{He},\alpha)$ study, especially in the previously unexplored excitation energy range of 2.5–12 MeV. From angular distribution measurements, transferred l values have been attributed to many discrete levels or groups of levels, and to 1-MeV-wide energy bins in the continuum region. Due to the high-energy resolution of the present experiment, 10 $l=4$, 12 $l=1$, and 16 $l=3$ peaks have been observed in the 2.5–6 MeV region. Furthermore, it has been shown that $l=1$ and $l=3$ neutron transfers both contribute to the excitation of the continuum below 12 MeV. Within the accuracy of the relative C^2S factors obtained in this experiment, it is found that the $1g_{\frac{9}{2}}$ and $2f-1p$ neutron-hole states are practically exhausted below 12 MeV. Based on the present measurements and some additional assumptions about the j values of the final levels, centroid values have been proposed for the various hole states.

In addition to the data obtained about the distribution of $1g_{\frac{9}{2}}$ and $1f-2p$ strength in ^{87}Sr , the present $(^3\text{He},\alpha)$ study gives strong evidence for some neutron-hole core-coupling states at low excitation energy, as their high-spin values prevent any configuration mixing. The experimental differential cross sections obtained for four low-lying high-spin states are well reproduced by CRC calculations assuming pure two-step processes, with the inelastic excitation of the core coupled to a $g_{\frac{9}{2}}$ neutron transfer, and spin and parity assignments could then be proposed from this analysis. Core-coupling mechanisms are also generally thought to be responsible for the fragmentation and damping of the inner-hole strengths observed in one-nucleon pickup experiments. It is hoped that the present data about ^{87}Sr could be usefully compared to further theoretical predictions.

ACKNOWLEDGMENTS

We would like to thank Professor Ch. Stoyanov for fruitful discussions. We also acknowledge the technical staff of the Orsay Tandem for the efficient running of the accelerator, and J. C. Artiges and P. Cohen for their help during the experiment.

*Present address: University of La Plata, La Plata, Argentina.

¹S. Gales, E. Hourani, S. Fortier, H. Laurent, J. M. Maison, and J. P. Schapira, Nucl. Phys. **A288**, 221 (1977).

²J. Van de Wiele, E. Gerlic, H. Langevin-Joliot, and G.

Duhamel, Nucl. Phys. **A297**, 61 (1978), and references cited therein.

³G. Duhamel, G. Perrin, J. P. Didelez, E. Gerlic, H. Langevin-Joliot, J. Guillot, and J. Van de Wiele, J. Phys. G **7**, 1415

- (1981).
- ⁴C. P. Massolo, S. Fortier, J. M. Maison, and M. N. Rao, *J. Phys. G* **8**, 361 (1982).
- ⁵J. Kasagi, G. M. Crawley, E. Kashy, J. Duffy, S. Gales, E. Gerlic, and D. Friesel, *Phys. Rev. C* **28**, 1065 (1983).
- ⁶Nguyen Dhin Thao, V. G. Soloviev, Ch. Stoyanov, and A. I. Vdovin, *J. Phys. G* **10**, 517 (1984).
- ⁷P. Luksch and J. W. Tepel, *Nucl. Data Sheets* **B27**, 389 (1979).
- ⁸R. G. Markham and R. G. H. Robertson, *Nucl. Instrum. Methods* **129**, 131 (1975).
- ⁹Internal Report IPNO-87-03, Orsay, 1987 (unpublished).
- ¹⁰P. D. Kunz (unpublished).
- ¹¹R. Stock and T. Tamura, *Phys. Lett.* **22**, 177 (1966).
- ¹²C. M. Perey and F. G. Perey, *At. Data Nucl. Data Tables* **17**, 1 (1976).
- ¹³H. Taketani *et al.*, *Nucl. Phys.* **A204**, 385 (1973).
- ¹⁴S. Fortier, E. Hourani, N. M. Rao, and S. Gales, *Nucl. Phys.* **A311**, 324 (1978).
- ¹⁵A. Stuirbrink *et al.*, *Z. Phys. A* **297**, 307 (1980).
- ¹⁶S. E. Arnell, A. Nilsson, and O. Stankiewicz, *Nucl. Phys.* **A241**, 109 (1975).
- ¹⁷H. P. Blok, W. R. Zimmerman, J. J. Kraushaar, and P. A. Batay-Csorba, *Nucl. Phys.* **A287**, 156 (1977).
- ¹⁸J. Picard, O. Beer, A. El Behay, P. Lopato, Y. Terrien, G. Vallois, and R. Schaeffer, *Nucl. Phys.* **A128**, 481 (1969).
- ¹⁹S. K. Basu and S. Chen, *Nucl. Phys.* **A220**, 580 (1974).
- ²⁰J. E. Kitching, *Z. Phys.* **258**, 22 (1973).
- ²¹S. M. Abecassis, J. Davidson, and M. Davidson, *Phys. Rev. C* **22**, 2237 (1980).